Zero-temperature magnetic ordering in the inhomogeneously frustrated quantum Heisenberg antiferromagnet on a square lattice

Johannes Richter
Institut für Theoretische Physik, Technische Universität Magdeburg, Postfach 4120, D-3010 Magdeburg, Germany
(Received 27 July 1992)

We examine the influence of homogeneous and inhomogeneous frustration on the ground-state ordering of the spin-$\frac{1}{2}$ J_1-J_2 Heisenberg antiferromagnet on a square lattice with $N=16$ and $N=20$ sites. For a critical value of frustration $J_2^{\rm crit}\approx 0.4J_1$ the conventional collinear antiferromagnetic long-range order is expected to break down in the homogeneously frustrated system. This critical frustration is drastically decreased by inhomogeneities simulating doping; we find $J_2^{\rm crit}\approx 0.15J_1$, which is quite realistic for the situation in slightly doped cuprate superconductors. In the region of strong frustration a quantum spin-liquid state is realized without conventional collinear ordering. The properties of this quantum spin liquid are still under controversial discussion. Three different possibilities of a noncollinear ordering in the strongly frustrated region ($J_2\approx 0.5J_1$) are discussed: A dimerized (or spin-Peierls) state, a state with scalar chiral ordering, and a state with enhanced vector chiral correlations. In particular, owing to the possibility of excitations with fractional statistics and owing to experimental investigations of broken reflection symmetry and parity the symmetry properties of the chiral order parameters are of interest. The scalar chirality is odd under time reversal and two-dimensional reflection, whereas the vector chirality conserves the time-reversal symmetry. We find evidence for a vector chiral ordering as well as for a spin-Peierls state. These vector chiral correlations can be enhanced by local inhomogeneities (holes), whereas the spin-Peierls state is suppressed.

I. INTRODUCTION

In recent times the two-dimensional (2D) quantum spin Heisenberg antiferromagnet (AFM) has attracted a great deal of attention in connection with the antiferromagnetic properties of materials with high-temperature superconductivity. In the Cu-O planes being responsible for the superconductivity in high-T_c materials, the Cu spin is 1/2, the in-plane exchange is strong [more than 1000 K in La_2CuO_4 (Ref. 1)] and exceeds the off-plane exchange substantially. The anisotropy in the spin space is small. Hence, in the insulating phase the interacting Cu spins should be well described by an $S=1/2$ Heisenberg AFM on the square lattice. For example, La_2CuO_4 shows antiferromagnetic long-range order (LRO) in the undoped insulating case with a Néel temperature of about 300 K.[2] Doping the material with a small amount of Ba or Sr, the system remains insulating but the magnetic LRO vanishes,[3] suggesting a great sensitivity of LRO to defects in quasi-2D AFM.

Although according to Mermin and Wagner's theorem[4] magnetic LRO at finite temperatures is excluded for the isotropic Heisenberg magnet in 2D, numerous theoretical ground-state (GS) investigations of 2D Heisenberg AFM confirm the existence of LRO at $T=0$ (e.g., Refs. 5–15 and the review in Ref. 16). However, a proof for antiferromagnetic LRO in the GS of the Heisenberg AFM is available at present only for $S\geq 1$ (Refs. 17,18) in the isotropic case or for an anisotropic exchange in the extreme quantum case $S=1/2$ (Ref. 19 and references therein).

Hence the anomalously fast disappearance of antiferromagnetic LRO by doping (e.g., for La_2CuO_4) is certainly related to the quasi-2D character of the spin system and can be forced by different mechanisms.

(i) There is a certain degree of antiferromagnetic next-nearest-neighbor (NNN) exchange J_2 between the Cu spins of about 5–20% of the nearest-neighbor (NN) exchange J_1 (Refs. 20–23) which creates frustration. As argued in Ref. 24 this frustration could increase with doping.

(ii) Doping creates holes in the Cu-O plane which mainly occupy oxygen sites.[25,26] Since the exchange integral between neighbor Cu spins is dominated by a superexchange mechanism, the holes locally modify the bonds. According to Aharony and co-workers,[27] a local change from an antiferromagnetic to a strong ferromagnetic bond due to a hole is suggested (Aharony model), which introduces a plaquette frustration.[28,29] Alternatively, it was argued by Zhang and Rice[30] that a static hole is distributed over all four oxygen sites surrounding a certain copper site. The distributed hole and the copper spin form a local singlet state. This Zhang-Rice singlet could be simulated by cutting the oxygen mediated NN exchange coupling of that copper spin.

(iii) The holes are not fully localized at a definite oxygen site. The hopping processes of the hole create additional spin fluctuations.

We address our attention in this paper to (i) and (ii), and describe the AFM within the localized spin Heisenberg model. To discuss (iii) Hubbard-like models or the t-J model, taking into account electronic hopping, have to be used.

It is well known from spin glasses[31] that frustration influences magnetic LRO. For quantum spin systems this can be convincingly demonstrated by use of exactly solvable quantum spin chains. In the GS of the one-dimensional Heisenberg AFM[32,33] with NN exchange J_1 the spin correlation decays slowly following a $1/R$ power law. Introducing frustration by NNN exchange J_2 of strength $J_2=J_1/2$, the GS state is a valence bond state[34,35] for which the spin correlation is extremely short ranged.

The influence of frustrating NNN bonds J_2 for the Heisenberg spin-1/2 AFM on a square lattice is described by the so-called J_1-J_2 model,

$$H=J_1\sum_i(\mathbf{S}_i\cdot\mathbf{S}_{i+\hat{x}}+\mathbf{S}_i\cdot\mathbf{S}_{i+\hat{y}})+J_2\sum_i(\mathbf{S}_i\cdot\mathbf{S}_{i+\hat{x}+\hat{y}}+\mathbf{S}_i\cdot\mathbf{S}_{i+\hat{y}-\hat{x}})\ , \qquad (1)$$

where $\mathbf{S}_i$ denotes the spin-1/2 operator on site i and the $\hat{x}$ and $\hat{y}$ are unit lattice vectors in x and y directions.

The model (1) was discussed in several papers in recent times.[14,15,36–58] The main conclusions from these papers are as follows:

(i) There is some evidence that for a critical value (J_2^{crit}/J_1) the conventional collinear antiferromagnetic LRO breaks down. Though the calculations for (J_2^{crit}/J_1) are not very precise, a value of about 0.4 appears to be reasonable.[15,37]

(ii) For $J_2/J_1 \gtrsim 0.65$ the large J_2 creates collinear magnetic ordering with a columnwise arrangement of up and down spins. If J_2 further increases, an antiferromagnetic LRO arises within the initial sublattices.[43,15]

(iii) In the region of strong frustration $(J_2/J_1\approx 0.5)$ a quantum spin-liquid state could be realized without conventional collinear ordering. The properties of this quantum spin liquid are still controversial. For J_2 slightly above the critical value there are indications of a short-range resonating valence bond state with an exponentially decaying two-spin-correlation function.[41,46,48] However, more interesting is the suggestion of a noncollinear LRO put forward in several papers.[15,40,43,44,47,52–58] Three different possibilities are discussed: a dimerized (or spin-Peierls) state, a state with scalar chiral ordering, or a state with enhanced vector chiral correlations. In particular, owing to the possibility of excitations with fractional statistics (anyons)[40] and owing to experimental investigations of broken reflection symmetry and parity,[59–61] the symmetry properties of these states are of considerable interest.

Recently, the static and dynamic properties of the J_1-J_2 model were compared with corresponding properties of the t-J model.[62] While the static properties of both models are qualitatively similar, it is not surprising that a significant difference between both models was found for dynamic properties.

In the present paper we discuss static magnetic GS correlations and study the influence of localized holes simulated by ferromagnetic bonds (Aharony model) and by cutoff NN bonds (Zhang-Rice) in the J_1-J_2 model. We are interested in the influence of these additional inhomogeneities on the stability of conventional antiferromagnetic LRO as well as the formation of exotic types of order in the strongly frustrated region. Because the critical frustration $(J_2^{\text{crit}}/J_1)\approx 0.4$ for the breakdown of the AFM is too large, being realistic for materials with high-T_c superconduction, it is particularly interesting whether or not the static holes are able to reduce the critical J_2 drastically.

In the frustrated quantum Heisenberg model, Monte Carlo methods are difficult to apply because of the minus sign problem. Therefore we use as the standard technique (Refs. 5,15,46–48,53,54) the Lanczos procedure for the exact diagonalization of clusters of 16 and 20 sites on the square lattice.

II. THE J_1-J_2 MODEL WITH INFINITE RANGE INTERACTIONS

Let us start with a simple soluble version of the spin-$\frac{1}{2}$ J_1-J_2 model,

$$H=J_1\sum_{i\in A,j\in B}\mathbf{S}_i\cdot\mathbf{S}_j+J_2\sum_{i,j\in A}\mathbf{S}_i\cdot\mathbf{S}_j+J_2\sum_{i,j\in B}\mathbf{S}_i\cdot\mathbf{S}_j\ , \qquad (2)$$

which is a variant of a model first studied by Lieb and Mattis.[63] In contrast to (1) the interaction J_{ij} is equal to J_1 for all spin pairs (i,j) belonging to different sublattices A and B and equal to J_2 for all pairs belonging to the same sublattice of either A or B, independent of $\mathbf{R}_i$-$\mathbf{R}_j$. Then H can be expressed by the squares of the total spins:

$$\mathbf{S}=\sum_i\mathbf{S}_i,\quad \mathbf{S}_A=\sum_{i\in A}\mathbf{S}_i,\quad \mathbf{S}_B=\sum_{i\in B}\mathbf{S}_i\ . \qquad (3)$$

One finds

$$H=(1/2)J_1\mathbf{S}^2+(J_2\text{-}J_1/2)\mathbf{S}_A^2+(J_2\text{-}J_1/2)\mathbf{S}_B^2-J_2(3N/4)\ , \qquad (4)$$

where N is the total number of interacting spins. According to the first term in (4), the GS is a singlet $\mathbf{S}^2=0$ for antiferromagnetic $J_1>0$. The values of $\mathbf{S}_A$ and $\mathbf{S}_B$ in the GS depend on J_2. We consider frustration, i.e., competing antiferromagnetic $J_2>0$. For smaller values of frustration $J_2<0.5J_1$, both $\mathbf{S}_A^2$ and $\mathbf{S}_B^2$ are as large as possible, i.e., $\mathbf{S}_\alpha^2=(N/4)(N/4+1)$, for strong frustration $J_2>0.5J_1$ we have $\mathbf{S}_\alpha^2=0$ $(\alpha=A,B)$. At $J_2=J_1/2$ (maximum of frustration) the ground-state energy is degenerated with respect to $\mathbf{S}_A^2$ and $\mathbf{S}_B^2$.

Now we can calculate the spin-spin correlation functions in the GS. One finds for $J_2<0.5J_1$:

$$\langle\mathbf{S}_i\mathbf{S}_j\rangle|_{i,j\in A}=\langle\mathbf{S}_i\mathbf{S}_j\rangle|_{i,j\in B}=1/4\ , \qquad (5a)$$

$$\langle\mathbf{S}_i\mathbf{S}_j\rangle|_{i\in A,j\in B}=-(1/4+1/N)\ , \qquad (5b)$$

and for $J_2=0.5J_1$:

$$\langle\mathbf{S}_i\mathbf{S}_j\rangle|_{i,j\in A}=\langle\mathbf{S}_i\mathbf{S}_j\rangle|_{i,j\in B}=\langle\mathbf{S}_i\mathbf{S}_j\rangle|_{i\in A,j\in B}=-3/[4(N-1)]\ , \qquad (6)$$

and for $J_2>0.5J_1$:

$$\langle\mathbf{S}_i\mathbf{S}_j\rangle|_{i,j\in A}=\langle\mathbf{S}_i\mathbf{S}_j\rangle|_{i,j\in B}=-(3/2)[1/(N-2)]\ , \qquad (7a)$$

$$\langle \mathbf{S}_i \mathbf{S}_j \rangle |_{i \in A, j \in B} = 0 \tag{7b}$$

(i.e., for $J_2 > 0.5J_1$, the sublattices A and B are effectively decoupled).

For finite systems, antiferromagnetic LRO can be described by the square of the sublattice magnetization of one spin component:

$$M_s^2 = \left\langle \left[\frac{1}{N} \sum_{i=1}^{N} \tau_i S_{iz} \right]^2 \right\rangle, \quad \tau_{i \in A} = +1, \quad \tau_{i \in B} = -1 \ . \tag{8}$$

For dominating J_2, an order parameter

$$M_{s,\alpha}^2 = \left\langle \left[\frac{1}{N/2} \sum_{i_\alpha = 1}^{N/2} \tau_{i,\alpha} S_{iz} \right]^2 \right\rangle, \quad \tau_{i,\alpha} = \pm 1, \alpha = A, B \tag{9}$$

is relevant (see Sec. III B), which describes an antiferromagnetic order within the initial sublattices A and B. $\tau_{i,\alpha}$ is the corresponding staggered factor. We notice that in a singlet GS the x and y components contribute with the same value to the square of the sublattice magnetization. Furthermore, we can write M_s^2 as

$$M_s^2 = -[4/(3N^2)] \langle \mathbf{S}_A \mathbf{S}_B \rangle \ , \tag{10}$$

indicating that in a singlet GS the sublattice magnetization is related to the coupling between the total spins of the two sublattices A and B.

From Eqs. (5)–(7) one obtains for M_s^2

$$M_s^2 = (1/3)(1/4 + 1/N); \quad J_2 < 0.5J_1 \ , \tag{11}$$

$$M_s^2 = (1/4)\{1/N + 1/[N(N-1)]\}; \quad J_2 = 0.5J_1 \ , \tag{12}$$

$$M_s^2 = 0, \quad M_{s,\alpha}^2 = (1/2)\{1/N + 1/[N(N-2)]\}, \quad J_2 > 0.5J_1 \ . \tag{13}$$

In the limit of large N the correlation functions as well as the sublattice magnetizations approach the molecular field values. As expected, the frustration acts against the antiferromagnetic ordering; the spin-spin correlation as well as the sublattice magnetization vanish in the thermodynamic limit. For finite N, the quantum fluctuations are present and yield finite antiferromagnetic correlations even in the strongly frustrated case. Furthermore Eqs. (5)–(7), (11)–(13) contain the finite-size scaling rules for the order parameters of the model (2). In contrast to the $1/\sqrt{N}$ scaling found in the 2D Heisenberg AFM for M_s^2 (Refs. 11,15,64) the leading term here is $1/N$. In the frustrated case, one has quadratic corrections indicating a possible sensitivity of finite-size scaling rules against frustration, particularly for small systems.

III. THE J_1-J_2 MODEL ON THE SQUARE LATTICE

We investigate now the GS of the model (1) for $N = 16$ and $N = 20$ sites with additional local defects of the Aharony type (local ferromagnetic bonds) and of the Zhang-Rice type (cutoff NN bonds of a certain spin). For the scaling of the energy we choose $J_1 = 1$ and consider four different bond configurations:

HS: homogeneous system without defects,

FM1: one ferromagnetic NN bond of strength $J_{\mathrm{fm}} = -J_1$,

FM2: two ferromagnetic NN bonds of strength $J_{\mathrm{fm}} = -J_1$,

ZR: one Zhang-Rice defect.

The configuration FM1 corresponds to a "hole" concentration of $1/2N$ and configurations FM2 and ZR to $1/N$. In the case of two ferromagnetic bonds (FM2) we choose the configuration with the lowest energy for small J_2 (see Fig. 1), i.e., both bonds belong to the same plaquette and are opposite each other (e.g., for $N = 16$, this configuration has the lowest energy for $J_2/J_1 < 0.65$). Clearly, the arrangements of ferromagnetic bonds in the x or alternatively, the y direction are physically equivalent. For the calculation of order parameters, unless we consider local quantities, we average over both arrangements. Additionally, to the FM2 configuration with the lowest energy, we considered an average over *all* configurations with two ferromagnetic bonds as well. However, this yielded qualitatively the same results as the lowest energy configuration and therefore we did not present them.

We notice that for finite J_2 the 20-site cluster has a symmetry other than the 16-site cluster (cf. Refs. 43,15). In particular, there is a level crossing for $N = 20$ at about $J_2 \approx 0.58$ for the homogeneous case, which influences the properties of the system in the vicinity of this point.

A. Ground-state energy

The frustration causes an energy increase induced both by unsatisfied bonds and by the reduction of the correlation strength of interacting spins. Therefore the maximum in the energy curve marks the region of strongest frustration and the deviation from the linear behavior in-

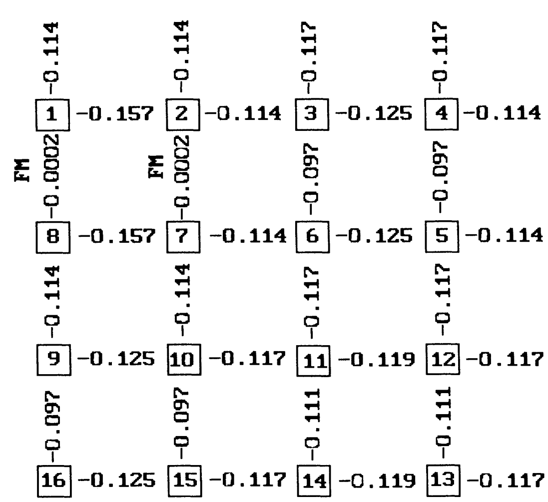

FIG. 1. Arrangement of sites and bonds for the 16-site cluster discussed in the paper. The numbers between the sites represent the nearest-neighbor spin correlation $\langle S_i^z S_j^z \rangle$ for the system with two ferromagnetic bonds (FM2) between sites 1 and 8 and sites 2 and 7, respectively.

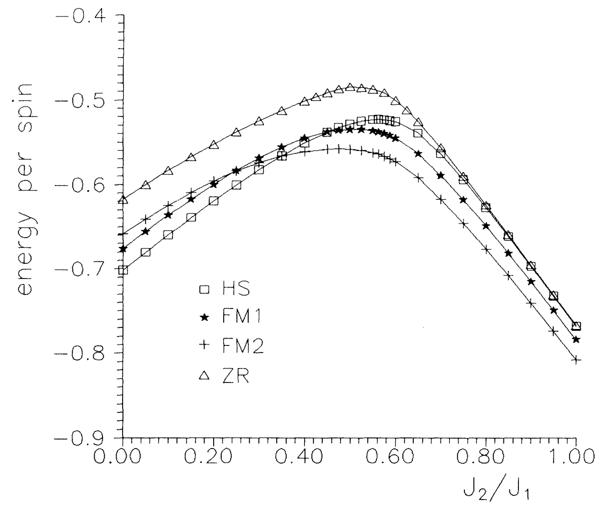

FIG. 2. Energy per spin vs J_2/J_1 for the homogeneous system (HS), the system with one ferromagnetic bond (FM1), two ferromagnetic bonds (FM2), and one Zhang-Rice defect (ZR) for $N=16$.

dicates a change in the relation between NN and NNN spin correlation. For the simple model (2) the energy depends linearly on J_2 with a kink at its maximum value at $J_2/J_1=0.5$. The energy for the 2D model (1) is drawn in Fig. 2. For small J_2, the homogeneously frustrated system has the lowest energy. The system with the Zhang-Rice defect has a higher energy since four NN bonds are missing. Moreover, there are level crossings at $J_2\approx0.5$ and $J_2\approx0.6$ for the ZR system, which will influence the order parameters in that region of J_2. For the systems with ferromagnetic bonds, the energy is increased by additional plaquette frustration, which creates weakly correlated unsatisfied bonds even for $J_2=0$ [cf. Fig. 1, bonds (1,8) and (7,2)]. The maximum of the energy is at $J_2/J_1\approx0.56$ for the homogeneous system, i.e., at slightly higher values than for model (2). However, it is shifted to smaller J_2 values by the defects. For larger J_2 the two sublattices become more and more decoupled for the homogeneous system and the ZR system as it is shown by the NN spin correlation in Fig. 3(a). For systems with ferromagnetic bonds, the averaged NN spin correlation is close to the value of the homogeneous system, but as shown by Fig. 3(b) the correlation strongly varies from bond to bond and there is a magnetic coupling between the two sublattices yielding an energy gain for $J_2>0.5$ (Fig. 2).

B. Conventional antiferromagnetic LRO

First we discuss the averaged pair-correlation function $\langle S_i^z S_j^z\rangle$, which is dependent upon the separation r_{ij} for different values of frustration. Obviously, the frustration reduces the spin-spin correlation drastically. In particular, for longer distances the correlation is almost completely suppressed for strong frustration [HS, $J_2=0.5$, Fig. 4(a)]. If we introduce additional defects [Figs. 4(b)–4(d)] this tendency is increased and the suppression of longer-distance correlations is obtained for clearly lower values of J_2. It seems to be evident that frustration is able to destroy long-range correlations for values of J_2 significantly lower than 0.5.

However, increasing J_2 beyond 0.6, the spin correlations $\langle S_i^z S_j^z\rangle$ for lattice points i and j belonging to the same sublattice A or B reappear [cf. (Figs. 4(e),4(f)], whereas the intersublattice correlations are drastically diminished. This indicates an antiferromagnetic ordering within the initial sublattices for large J_2.

Let us now discuss the global antiferromagnetic long-range order. For that we use as order parameters the square of the sublattice magnetization M_s^2 [Eq. (8)] to describe the conventional LRO and $M_{s,\alpha}^2$ [Eq. (9)] to describe antiferromagnetic LRO within the initial sublattices. M_s^2 and $M_{s,\alpha}^2$ are shown in Fig. 5. Obviously, there are indications for a quantum spin-liquid region around $J_2\approx0.5$ where both order parameters describing conven-

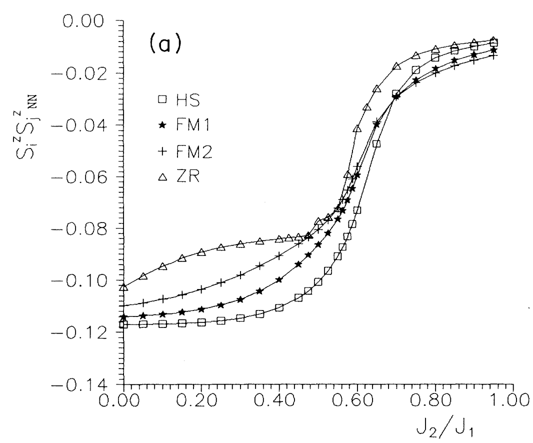

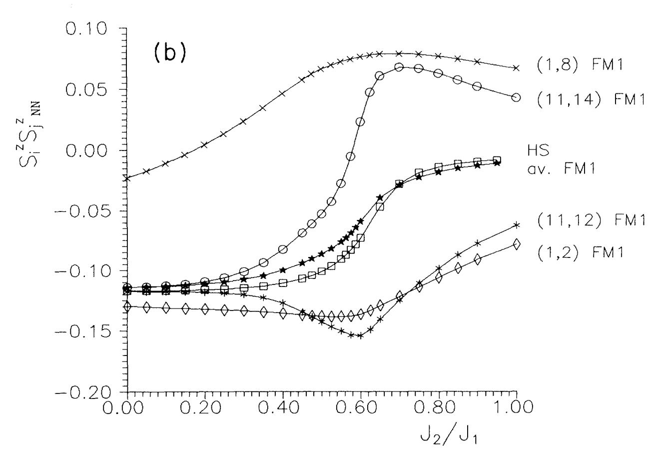

FIG. 3. Nearest-neighbor spin correlation $\langle S_i^z S_j^z\rangle$ vs J_2/J_1 for $N=16$. (a) Averaged values over all nearest-neighbor bonds. (b) Local values for the system with one ferromagnetic bond (FM1) between sites 1 and 8 (for the arrangement of sites cf. Fig. 1). Local correlations are presented for bonds both far from and close to the defect. For comparison the averaged value for FM1 and the value for HS are shown.

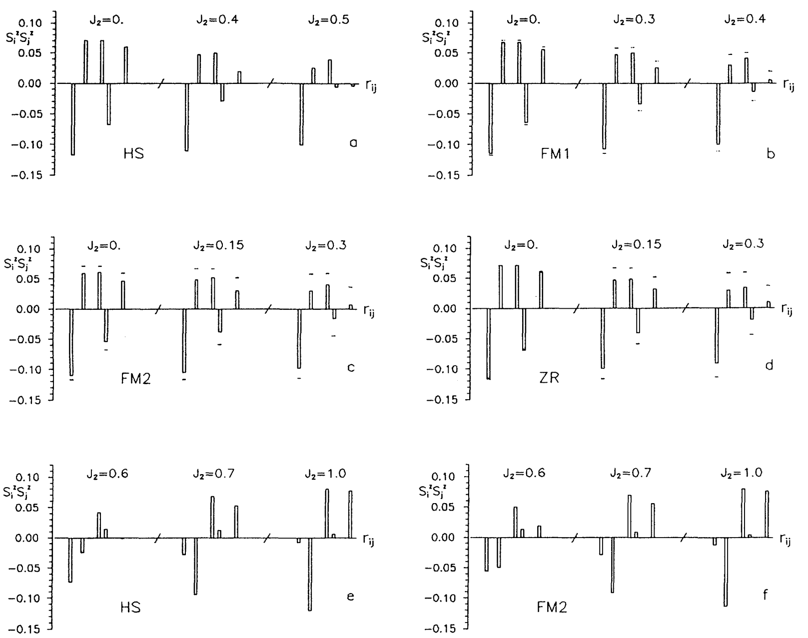

FIG. 4. Histogram of the averaged pair-correlation function $\langle S_i^z S_j^z \rangle$ dependent upon the spin separation r_{ij} for $N=16$ and various values of J_2. The columns belong to separations a, $\sqrt{2}\,a$, $2a$, $\sqrt{5}\,a$, and $\sqrt{8}\,a$ (a is the lattice separation). In b, c, and d the additional dots on the tops of the columns indicate the corresponding values of the homogeneous system. For the abbreviations HS, FM1, FM2, ZR see Fig. 2.

tional collinear LRO are very small.

The influence of the defects on the order-parameter $M_{s,\alpha}^2$ is weak [cf. Figs. 4(e) and 4(f)]. There is only a small shift of the critical J_2 values where the antiferromagnetic LRO within the initial sublattice occurs. Nevertheless, there is a difference between the systems with (FM1, FM2) and without ferromagnetic bonds (HS, ZR), the antiferromagnetic orders within the initial sublattices are coupled to each other by the ferromagnetic bonds, whereas they are almost decoupled for HS and ZR [cf. Fig. 3(b)].

More interesting is the order parameter M_s^2 which is relevant for small frustration. As discussed in the Introduction M_s^2 is expected to vanish in the thermodynamic limit at $J_2 \approx 0.4$ [for the homogeneously frustrated model (HS)].[15,37] This is confirmed by the pair correlation shown in Fig. 4(a). This critical $J_2 \approx 0.4$ is clearly too large to be relevant for the breakdown of AFM in cuprate superconductors. But as demonstrated by the pair correlation in Fig. 4 and M_s^2 in Fig. 5, the critical value can be drastically decreased by the defects, i.e., the quantum spin-liquid region is broadened by the defects. In Fig. 6 we present the M_s^2 curves for HS, FM1, and FM2 with rescaled values for J_2 in the relevant region of $J_2 \approx 0.4$ and find an effective reduction of J_2 of about 0.1

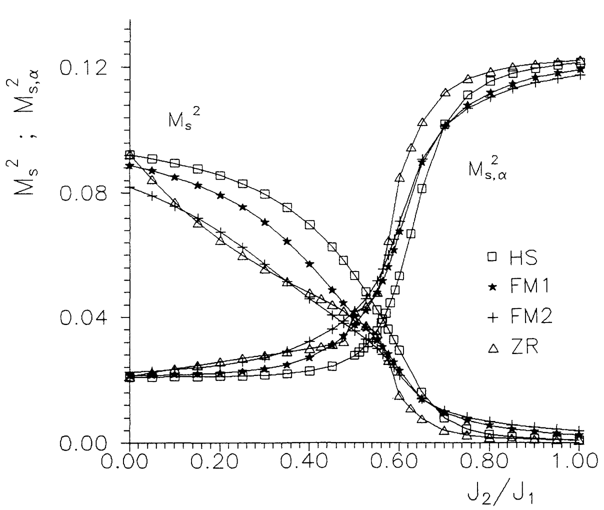

FIG. 5. Sublattice magnetizations M_s^2 and $M_{s,\alpha}^2$ ($\alpha=A,B$) [see Eqs. (8) and (9)] vs J_2/J_1 for $N=16$.

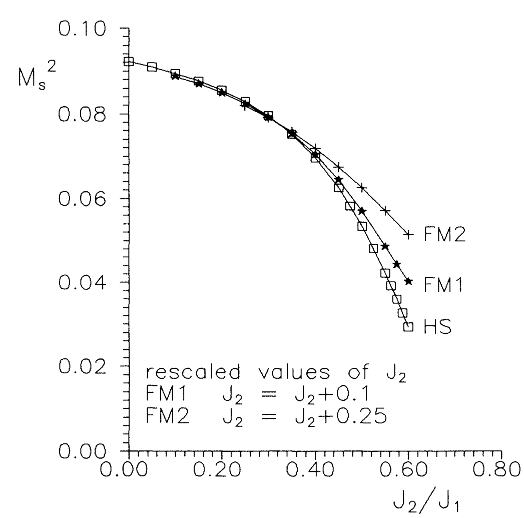

FIG. 6. Sublattice magnetization M_s^2 vs rescaled values of J_2 for $N=16$.

and 0.25, respectively. A resulting value of $J_2^{\rm crit} \approx 0.15$ in the latter case is, however, quite realistic in the cuprates. As estimated in the undoped material,[20–23] a $J_2 \approx 0.05 - 0.2$ may already be present.

Owing to the defects, the magnetic ordering is inhomogeneous as can be seen in Fig. 1. We can look for the square of the *local* sublattice moment,

$$M_{s,i}^2 = \left\langle \frac{1}{N} \sum_{j=1}^{N} \tau_i \tau_j S_{iz} S_{jz} \right\rangle ; \qquad M_s^2 = \frac{1}{N} \sum_{i=1}^{N} M_{s,i}^2 , \tag{14}$$

which is drawn in Fig. 7 for FM1. Site 1 is close to the defect and site 11 is far from the defect. For comparison the averaged sublattice magnetization and the sublattice magnetization for the HS are shown. We see clearly that the magnetic order is inhomogeneously distributed over the system, nevertheless the local moment of site 11 (far from the defect) is still lower than the value for the HS, indicating that the topological defect alters the magnetic order not only in its direct vicinity.

To demonstrate that similar effects as discussed above for $N=16$ are realized for $N=20$ also, we compare in Fig. 8, the sublattice magnetizations for HS and FM2. However, we notice that the finite-size scaling for M_s^2 discussed in several papers for the unfrustrated Heisenberg-AFM[5,9,15,64] is violated for $J_2 \gtrsim 0.3$. As discussed in Sec. II, care has to be taken if scaling rules of the unfrustrated systems are applied to frustrated ones.

Let us now discuss in more detail the ground-state properties in the strongly frustrated region $J_2 \approx 0.5$, where no conventional magnetic order in the pair correlation is present.

C. Chiral order

One very interesting candidate for an unconventional ordering in the strongly frustrated region is the chiral order. The chirality operator has to measure the handiness of a plaquette of spins. However, the definition of the chirality for spin system is not unique. In the context of the anyon theory of high-T_c superconductivity, Wen, Wilczek, and Zee[40] proposed the triple scalar product of three spins,

$$E_{ijk} = \mathbf{S}_i(\mathbf{S}_j \times \mathbf{S}_k) , \tag{15}$$

as the chirality operator of a triangular plaquette. This is usually called scalar chirality (cf. Refs. 44,52). However, starting in 1977 with Villains papers[65] on frustrated spin systems, a vector chirality was discussed in many other papers (cf. Ref. 44 and references therein). This vector chirality is defined as

$$\mathbf{F}_{ijk} = (\mathbf{S}_i \times \mathbf{S}_j + \mathbf{S}_j \times \mathbf{S}_k + \mathbf{S}_k \times \mathbf{S}_i) . \tag{16}$$

Furthermore, Caspers and Tielen[66] proposed a vector chirality parameter $\mathbf{G}_{ijk}$, which is related to the scalar chirality E_{ijk} by

$$\mathbf{G}_{ijk} = (\mathbf{S}_i + \mathbf{S}_j + \mathbf{S}_k) E_{ijk} . \tag{17}$$

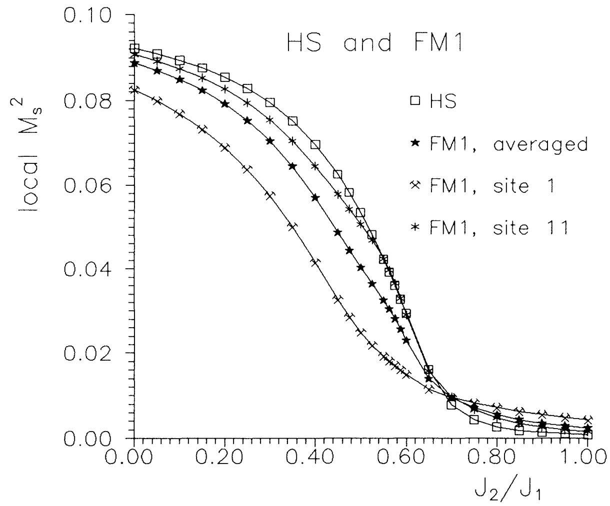

FIG. 7. Local sublattice magnetization $M_{s,i}^2$ for the system with one ferromagnetic bond between sites 1 and 8 (FM1) and $N=16$ (for the arrangement of sites cf. Fig. 1). For comparison the averaged values for FM1 and the value for HS are shown.

However, in the $S=1/2$ case considered here, both definitions of the vector chirality are identical;

$$\mathbf{G}_{ijk} = \tfrac{1}{4} \mathbf{F}_{ijk} . \tag{18}$$

Recently, Kawabayashi and Suzuki[44] found a Mermin-Wagner-like theorem for the vector chirality in 2D systems.

As for the sublattice magnetization we can choose one component of $\mathbf{G}_{ijk}$ arbitrarily for a singlet ground state. The z component considered here can be written as

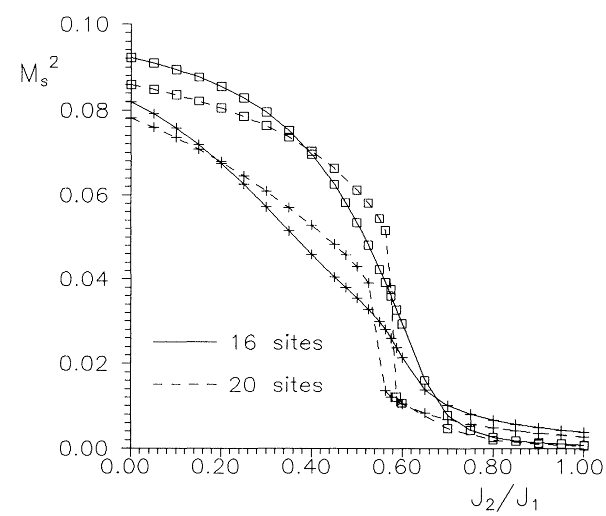

FIG. 8. Sublattice magnetization M_s^2 vs J_2/J_1 for the homogeneous system (HS, squares), and the system with two ferromagnetic bonds (FM2, crosses) with $N=16$ and $N=20$.

$$Z_{ijk} = 8(\mathbf{e}_z \cdot \mathbf{G}_{ijk}) = i[(S_i^+ S_j^- - S_i^- S_j^+) + (S_j^+ S_k^- - S_j^- S_k^+) + (S_k^+ S_i^- - S_k^- S_i^+)] , \quad (19)$$

which describes a spin current around the plaquette (i,j,k).

Obviously, the scalar and the vector chirality have different time-reversal symmetries; the first one is odd and the second one even.

The interpretation of E_{ijk} and Z_{ijk} as chirality operators can be illustrated by considering an isolated triangular plaquette. The quantities which commute with the Heisenberg-Hamiltonian of that triangle and with each other are the square of the total spin $(\mathbf{S}_1+\mathbf{S}_2+\mathbf{S}_3)^2$, the z component of the total spin $(S_{1z}+S_{2z}+S_{3z})$, and E_{123} from (15) or, alternatively, Z_{123} from (19). Hence the fourfold-degenerate ground state $|\phi\rangle$ of the antiferromagnetic plaquette can be characterized by the quantum numbers $E_0=-3/4J$, $S=1/2$, $S_z=\pm 1/2$ (Kramer's degeneracy) and the chirality (or rotational symmetry) of the state $C=\pm\sqrt{3}/4$,[66,67] i.e., the ground states can be divided into two classes of different chiralities. Applying E_{123} on the ground states, we find $E_{123}|E_0,S,S_z,C\rangle = 2S_zC|E_0,S,S_z,C\rangle$, i.e., E_{123} measures the product of S_z and C. Otherwise the application of Z_{123} on the ground state yields $Z_{123}|E_0,S,S_z,C\rangle = 16S_z^2C|E_0,S,S_z,C\rangle = 4C|E_0,S,S_z,C\rangle$, i.e., Z_{123} measures C alone.

As pointed out in Ref. 56 an order parameter of type (16) resembles the formerly discussed twist order parameter[43,47] with additional vector products along a diagonal direction.

Using Eq. (19) an order parameter

$$Z = \left\langle \left[\frac{1}{2N} \sum_i (Z_{i,i+\hat{x},i+\hat{x}+\hat{y}} - Z_{i,i+\hat{x}+\hat{y},i+\hat{y}}) \right]^2 \right\rangle \quad (20)$$

was discussed in Ref. 54. In (20) $\hat{x}$ and $\hat{y}$ are unit lattice vectors in the x and y direction. As pointed out in Ref. 54 this order parameter shows a significant enhancement in the strongly frustrated region of the J_1-J_2 model with 16 and 20 sites.[54] We show Z in Fig. 9 for HS, FM1, and FM2, and ZR. Due to the ferromagnetic bonds, the order parameter is increased (drastically for $N=16$, slightly for $N=20$) and the maximum is shifted to slightly smaller values of J_2. The reason for this enhancement of vector chiral correlations might be an additional tilting of spins in the vicinity of the defects. The ZR defect suppresses Z for $J_2 \lesssim 0.5$, but then the system changes over to a state of high Z for a small region of $0.5 \lesssim J_2 \lesssim 0.6$. We conclude that defects and particularly

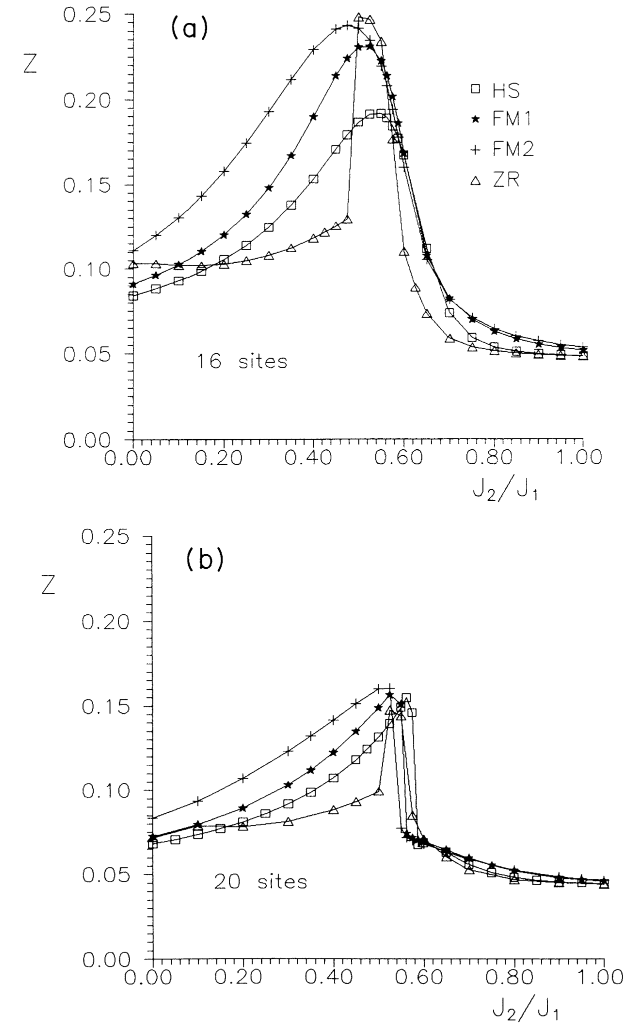

FIG. 9. Vector chiral order parameter Z [cf. Eq. (20)] vs J_2/J_1 for $N=16$ (a) and $N=20$ (b).

ferromagnetic bonds may favor a tendency towards enhanced vector chiral correlations in the ground state.

An order parameter based on the triple scalar product was discussed for $N=16$ and $N=20$ by Dagotto, and Poilblanc and co-workers.[43,53] Initially they argued that there is no evidence of enhanced scalar chiral correlations in the J_1-J_2 model.[43] This was confirmed by an effective-field calculation of Kawabayshi and Suzuki.[52] However, recently Poilblanc *et al.* studied the scalar chirality with different symmetries.[53] They found a strong increase of

$$T_A = \left\langle \left[\frac{1}{N} \sum_i (E_{i,i+\hat{x},i+\hat{x}+\hat{y}} + E_{i+\hat{x}+\hat{y},i+\hat{y},i} + E_{i+\hat{y},i,i+\hat{x}} + E_{i+\hat{x},i+\hat{x}+\hat{y},i+\hat{y}}) \right]^2 \right\rangle \quad (21)$$

for $N=16$. The parameter T_A has A_2 symmetry and is odd both under time-reversal (T) and parity (P) and therefore most interesting for the anyon physics. Confusingly, they found a very large parameter

$$T_B=\left\langle \left[\frac{1}{N}\sum_i (E_{i,i+\hat{x},i+\hat{x}+\hat{y}}+E_{i+\hat{x}+\hat{y},i+\hat{y},i}-E_{i+\hat{y},i,i+\hat{x}}-E_{i+\hat{x},i+\hat{x}+\hat{y},i+\hat{y}}\right]^2\right\rangle \tag{22}$$

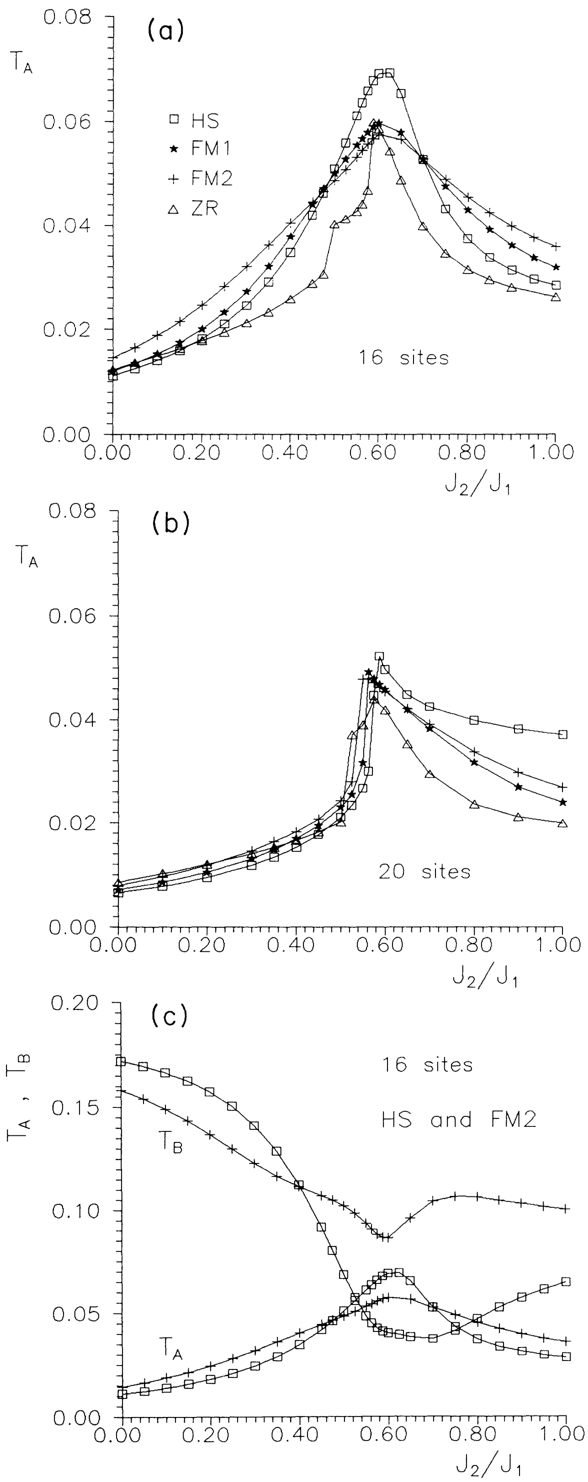

FIG. 10. Scalar chiral order parameters vs J_2/J_1. (a) Parameter T_A [cf. Eq. (21)] with A_2 symmetry for $N=16$. (b) T_A for $N=20$. (c) Comparison of T_A and the parameter T_B with B_1 symmetry [cf. Eq. (22)] for $N=16$.

for B_1 symmetry also, which clearly is even larger than T_A and has, surprisingly, a maximum value for the conventional unfrustrated Heisenberg AFM (i.e., $J_2=0$). Hence it was unclear whether the maximum in T_A in the frustrated region can be really interpreted as an indication of a ground state with broken scalar chiral symmetry. Let us look for the influence of defects on T_A and T_B. The results are presented in Fig. 10. Obviously, the defects diminish the maximum in T_A. This tendency is obtained for $N=16$ [Fig. 10(a)] and $N=20$ [Fig. 10(b)]. On the other hand, the minimum in T_B is strongly increased by the defects [Fig. 10(c)]. We argue that a state with scalar chiral order with A_2 symmetry, i.e., with broken T and P symmetry, in the J_1-J_2 model seems to be doubtful and is additionally disfavored by defects.

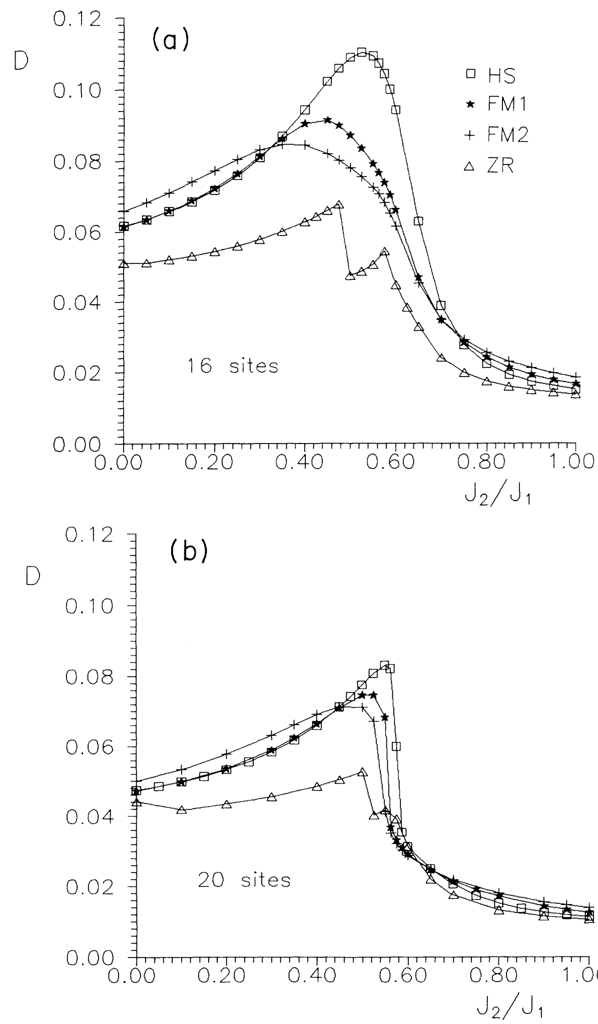

FIG. 11. Dimer order parameter D [cf. Eq. (23)] vs J_2/J_1 for (a) $N=16$ and (b) $N=20$.

D. Dimer order

Another candidate for unconventional ordering in the spin-liquid region of the J_1-J_2 model is a columnwise arrangement of spin dimers (singlet states of two spins). The order parameter used in the literature is[43,47,53–55]

$$D=2\left\langle \left[\frac{1}{N}\sum_i (-1)^{i_x}\mathbf{S}_i\cdot\mathbf{S}_{i+\hat{x}}\right]^2\right\rangle , \tag{23}$$

where i_x is given by the lattice vector $\mathbf{R}_i=(i_x,i_y)$ of the site i. This operator measures the long-range phase coherence of singlets along columns in the y direction. It was shown[43,54] that this dimer order parameter has a maximum for $N=16$ and $N=20$ for strong frustration almost at the same J_2 value as Z from Eq. (20). However, the enhancement of D caused by frustration was found to be lower than the enhancement of Z.[54] We now consider the influence of defects on D in Fig. 11 and find that defects strongly suppress dimer order. This is not surprising since defects certainly act against singlet formation.

E. Collinear state

Let us now turn to J_2 values above the quantum spin-liquid region discussed in the previous two sections. We know that for large J_2 a conventional antiferromagnetic LRO with a four-sublattice structure reappears [order-parameter $M^2_{s,\alpha}$ cf. Sec. B]. For $J_2 \gtrsim 0.65$ immediately above the quantum spin-liquid area, another collinear ordering with a columnwise arrangement of up and down spins is favored.[43,53,15] However, this type of ordering is related to the four-sublattice AFM since the corresponding columnwise Ising states are Néel states of the four-sublattice AFM. But otherwise, contrary to $M^2_{s,\alpha}$, the collinear column order is a state with important nearest-neighbor correlations and should be realized for J_2 values where $\langle \mathbf{S}_i\mathbf{S}_j\rangle$ for nearest neighbors is not yet too small (cf. Fig. 3).

We consider the order parameter[53,15]

$$C=\left\langle \left[\frac{1}{2N}\sum_i (\mathbf{S}_i\cdot\mathbf{S}_{i+\hat{x}}+\mathbf{S}_i\cdot\mathbf{S}_{i-\hat{x}} -\mathbf{S}_i\cdot\mathbf{S}_{i+\hat{y}}-\mathbf{S}_i\cdot\mathbf{S}_{i-\hat{y}})\right]^2\right\rangle . \tag{24}$$

Results for C are shown in Fig. 12. We see that the maximum of C is at $J_2 \approx 0.67$ for the homogeneous system (HS) where $M^2_{s,\alpha}$ is still small. We find a slight shift of the maximum to smaller J_2 caused by defects. But the influence of inhomogeneities on C is rather small, which corresponds to the findings for $M^2_{s,\alpha}$ in Fig. 5.

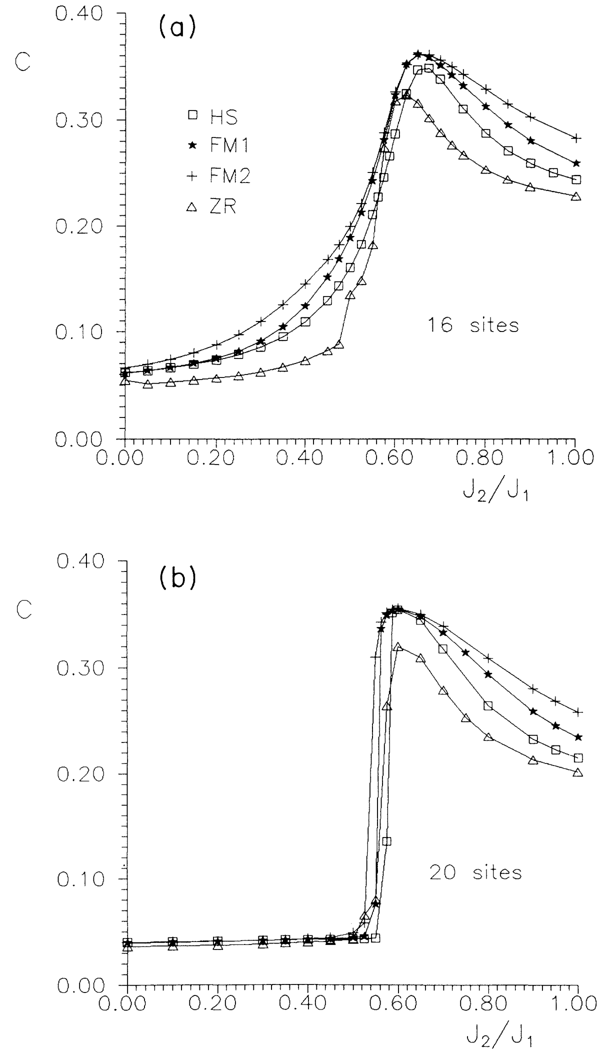

FIG. 12. Collinear order parameter C [cf. Eq. (24)] vs J_2/J_1 for (a) $N=16$ and (b) $N=20$.

IV. PHASE DIAGRAM AND CONCLUSIONS

What can we conclude from the discussion of several order parameters for the phase diagram for the two-dimensional J_1-J_2 model? To discuss this question, we present in Fig. 13 the calculated order parameters scaled by their maximum values. This allows us to find out the possible regions of different orders.

It is well known that we have conventional antiferromagnetic LRO for small J_2 (order-parameter M^2_s, two sublattices) and large J_2 (order-parameter $M^2_{s,\alpha}$ four sublattices). For intermediate values there is a quantum spin-liquid state which may have very interesting and complex properties. The critical frustration J_2/J_1 for which the two-sublattice antiferromagnetic order breaks down strongly depends on defects. In the homogeneous system, a critical J_2 of about 0.4 seems to be reasonable. Static inhomogeneities of low concentration may decrease the critical J_2 drastically up to values of about 0.15. Hence the region of the quantum spin liquid is considerably enlarged. We note that J_2 values of about 0.15 are quite reasonable for the slightly doped cuprate super-

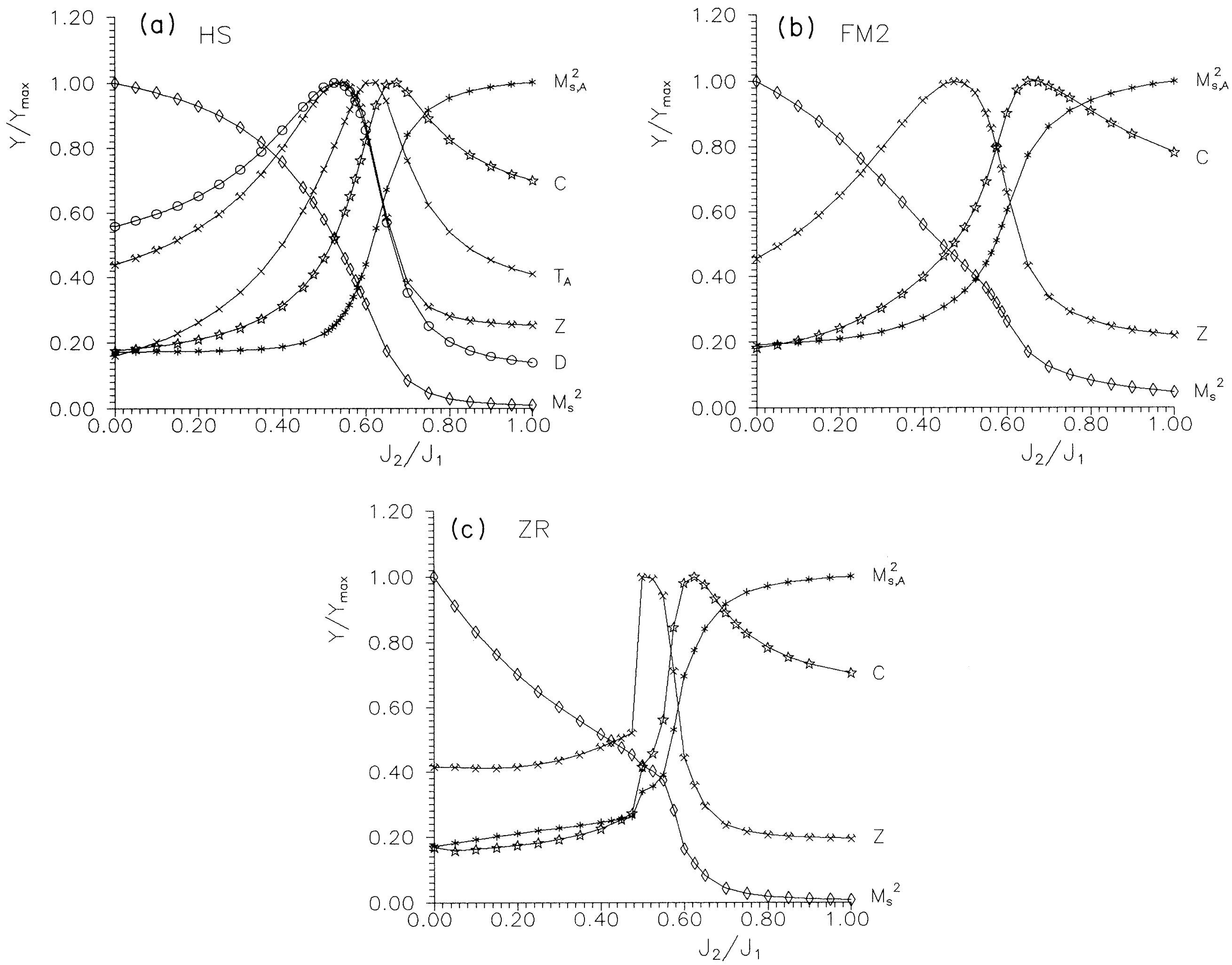

FIG. 13. Comparison of order parameters M_s^2, $M_{s,\alpha}^2$ ($\alpha = A,B$) [see Eqs. (8) and (9)], Z [cf. Eq. (20)], T_A [cf. Eq. (21)], D [cf. Eq. (23)], and C [cf. Eq. (24)] scaled by its maximum values for (a) the homogeneous system HS, (b) the system with two ferromagnetic inhomogeneities FM2, and (c) with a Zhang-Rice defect ZR. For FM2 and ZR we omitted T_A and D, because they seem to be less relevant.

conductors. But which properties have this quantum spin liquid? Doubtless there are indications of noncollinear ordering, described by an order parameter going beyond a simple pair-correlation description. For the homogeneous system without defects several candidates compete: dimer, vector chiral, and scalar chiral [see Fig. 13(a)]. To decide which of them has to be favored is difficult, but we can clearly argue that defects created by doping suppress dimer and scalar chiral ordering. But the vector chiral correlations may even be enhanced by defects. The zero-temperature phase diagram of the inhomogeneously frustrated J_1-J_2 model suggested by Fig. 13(b) and 13(c) may be described as follows: there is a small region of low frustration J_2 where a conventional but slightly disordered two-sublattice AFM exists. Increasing J_2 in this region is followed by a presumably short-range ordered, i.e., disordered phase. For strong frustration ($J_2 \approx 0.5$) there is a narrow region of noncollinear ordering which is well described by a vector chiral order parameter. Because this order parameter breaks the rotational symmetry in the spin space, this ground-state ordering implies gapless excitations. A further increase of J_2 to 0.6–0.65 yields a collinear state of rows of up and down spins which is a precursor of the four-sublattice antiferromagnetic state appearing for large J_2.

If we compare the systems with $N=16$ and $N=20$ we find that the general behavior of both is similar. However, in details there are differences, particularly for J_2 values in the vicinity of the level crossing point. Since this level crossing is specific for $N=20$, we argue that $N=16$ may be more representative for large systems.

Clearly it is necessary to consider larger N to support the conclusions given above. However, for finite J_2 the next cluster with full square lattice symmetry is $N=32$

and it is at the present time impossible to diagonalize $N=32$ for systems with defects breaking translational symmetry.

ACKNOWLEDGMENTS

The author would like to thank W. Weber and C. Gros (University of Dortmund) for stimulating discussions. This work has been supported by the Deutsche Forschungsgemeinschaft (Project No. Ri 615/1-1). Parts of the numerical calculations were done at the Hochleistungsrechenzentrum Jülich, Germany.

---

[1] G. Shirane, Y. Endoh, R. J. Birgeneau, M. A. Kastner, Y. Hidaka, M. Oda, M. Suzuki, and T. Murakami, Phys. Rev. Lett. **59**, 1613 (1987).

[2] S. K. Sinha, D. E. Moncton, D. C. Johnston, D. Vaknin, G. Shirane, and C. Stassis, J. Appl. Phys. **63**, 4015 (1988).

[3] D. Jerome, W. Kang, and S. S. P. Parkin, J. Appl. Phys. **63**, 4005 (1988).

[4] N. Mermin and H. Wagner, Phys. Rev. Lett. **17**, 1133 (1966).

[5] J. Oitmaa and D. D. Betts, Can. J. Phys. **56**, 897 (1978).

[6] D. A. Huse, Phys. Rev. B **37**, 2380 (1988).

[7] D. C. Mattis and C. Y. Pan, Phys. Rev. Lett. **61**, 463 (1988).

[8] E. Manousakis and R. Salvador, Phys. Rev. Lett. **60**, 840 (1988).

[9] P. Horsch and W. von der Linde, Z. Phys. B **72**, 181 (1988).

[10] K. W. Becker, H. Won, and P. Fulde, Z. Phys. B **75**, 335 (1989).

[11] J. D. Reger and A. P. Young, Phys. Rev. B **37**, 5978 (1988).

[12] H. Q. Ding and M. S. Makivic, Phys. Rev. Lett. **64**, 1449 (1991); M. S. Makivic and H. Q. Ding, Phys. Rev. B **43**, 3562 (1991).

[14] C. Buder and F. Mila, Europhys. Lett. **17**, 463 (1992).

[15] H. J. Schulz and T. A. L. Ziman, Europhys. Lett. **18**, 355 (1992).

[16] E. Manousakis, Rev. Mod. Phys. **63**, 1 (1991).

[17] E. J. Neves and J. F. Perez, Phys. Lett. **114A**, 331 (1986).

[18] I. Affleck, T. Kennedy, E. H. Lieb, and H. Tasaki, Commun. Math. Phys. **115**, 477 (1988).

[19] H. A. Wischmann and E. Müller-Hartmann, J. Phys. (Paris) **1**, 647 (1991).

[20] F. Annett, R. Martin, A. McMahan, and S. Satpathy, Phys. Rev. B **40**, 2620 (1989).

[21] D. Ihle and M. Kasner, Phys. Rev. B **42**, 4760 (1990).

[22] H. J. Schmidt and Y. Kuramoto, Physica C **167**, 263 (1990).

[23] A. Chubukov, E. Gagliano, and C. Balseiro, Phys. Rev. B **45**, 7889 (1992).

[24] M. Inui, S. Doniach, and M. Gabay, Phys. Rev. B **38**, 6631 (1988).

[25] V. J. Emery, Phys. Rev. Lett. **58**, 2794 (1987).

[26] A. Fujimori, E. Takayama-Muromachi, Y. Uchida, and B. Oaki, Phys. Rev. B **35**, 8814 (1987).

[27] A. Aharony, R. J. Birgeneau, A. Coniglio, M. A. Kastner, and H. E. Stanley, Phys. Rev. Lett. **60**, 1330 (1988); K. Lee and P. Schlottmann, Phys. Rev. B **42**, 4426 (1990).

[28] G. Toulouse, Commun. Phys. **2**, 915 (1977).

[29] J. Richter and S. Kobe, J. Phys. C **15**, 2193 (1982).

[30] F. C. Zhang and T. M. Rice, Phys. Rev. B **37**, 3759 (1988).

[31] K. Binder and A. P. Young, Rev. Mod. Phys. **58**, 801 (1986).

[32] H. Bethe, Z. Phys. **71**, 205 (1931).

[33] L. Hulthen, Arkiv Mat. Astron. Fys. **26a**, 11 (1938).

[34] C. K. Majumdar and D. K. Ghosh, J. Math. Phys. **10**, 1388 (1969).

[35] I. Affleck, J. Phys. Condens. Matter **1**, 3047 (1989).

[36] P. Chandra and B. Doucot, Phys. Rev. B **38**, 9335 (1988).

[37] J. E. Hirsch and S. Tang, Phys. Rev. B **39**, 2887 (1989).

[38] N. Read and S. Sachdev, Phys. Rev. Lett. **62**, 1694 (1989).

[39] E. Dagotto and A. Moreo, Phys. Rev. B **39**, 4744 (1989).

[40] X. G. Wen, F. Wilczek, and A. Zee, Phys. Rev. B **39**, 11 418 (1989).

[41] J. Richter, Phys. Lett. A **140**, 81 (1989).

[42] M. P. Gelfand, R. R. P. Singh, and D. A. Huse, Phys. Rev. B **40**, 10 801 (1989).

[43] E. Dagotto and A. Moreo, Phys. Rev. Lett. **63**, 2148 (1989).

[44] T. Kawarabayashi and M. Suzuki, Phys. Lett. A **143**, 17 (1990).

[45] P. Chandra, P. Coleman, and A. I. Larkin, Phys. Rev. Lett. **64**, 88 (1990).

[46] F. Figuereido, A. Karlhede, S. Kivelson, S. Sondhi, M. Rocek, and D. S. Rokhsar, Phys. Rev. B **41**, 4619 (1990).

[47] R. R. P. Singh and R. Narayanan, Phys. Rev. Lett. **65**, 1072 (1990).

[48] J. Richter, Z. Phys. B **79**, 403 (1990).

[49] A. F. Barabanov and O. A. Starykh, Pis'ma Zh. Eksp. Teor. Fiz. **51**, 271 (1990) [JETP Lett. **51**, 311 (1990)].

[50] J. H. Xu and C. S. Ting, Phys. Rev. B **42**, 6861 (1990).

[51] T. Einarson and H. Johanneson, Phys. Rev. B **43**, 5867 (1991).

[52] T. Kawarabayashi and M. Suzuki, J. Phys. Soc. Jpn. **60**, 825 (1991).

[53] D. Poilblanc, E. Gagliano, S. Bacci, and E. Dagotto, Phys. Rev. B **43**, 10 970 (1991).

[54] J. Richter, C. Gros, and W. Weber, Phys. Rev. B **44**, 906 (1991).

[55] A. Chubukov and Th. Jolicoeur, Phys. Rev. B **44**, 12 050 (1991).

[56] D. Poilblanc and E. Dagotto, Phys. Rev. B **45**, 10 111 (1992).

[57] J. Richter, C. Gros, and W. Weber, Phys. Rev. B **45**, 10 113 (1992).

[58] J. Richter, J. Magn. Magn. Mater. **104-107**, 505 (1992).

[59] K. B. Lyons, J. Kwo, J. F. Dillon, G. P. Espinosa, M. McGlashan-Powell, A. P. Ramirez, and L. F. Schneemeyer, Phys. Rev. Lett. **64**, 2949 (1990).

[60] S. Spielman, K. Fesler, C. B. Eom, T. H. Geballe, M. M. Fejer, and A. Kapitulnik, Phys. Rev. Lett. **65**, 123 (1990).

[61] H. J. Weber, D. Weitbrecht, D. Brach, A. L. Shelankov, H. Keiter, W. Weber, T. Wolf, J. Geerk, G. Linker, G. Roth, P. C. Splittgerber-Hünnekes, and G. Güntherodt, Solid State Commun. **76**, 511 (1990).

[62] S. Bacci, E. Gagliano, and F. Nori, Int. J. Mod. Phys. B **5**, 325 (1991).

[63] E. Lieb and D. C. Mattis, J. Math. Phys. **3**, 749 (1962).

[64] H. Neuberger and T. Ziman, Phys. Rev. B **39**, 2608 (1989).

[65] J. Villain, J. Phys. C **10**, 1717, 4793 (1977).

[66] W. J. Caspers and G. I. Thielen, Physica A **135**, 519 (1986).

[67] E. Fradkin, *Field Theories of Condensed Matter Systems* (Addison-Wesley, Reading, MA, 1991), p. 171ff.